First-principles modeling of resistance switching in perovskite oxide material

Sang Ho Jeon and Bae Ho Park[a),b)]
Department of Physics, Konkuk University, Seoul 143-091, Korea

Jaichan Lee
Department of Materials Science and Engineering, Sungkyunkwan University, Suwon 440-746, Korea

Bora Lee and Seungwu Han[a),c)]
Department of Physics, Ewha Womans University, Seoul 120-750, Korea

(Received 7 February 2006; accepted 3 June 2006; published online 25 July 2006)

We report a first-principles study on $SrRuO_3/SrTiO_3$ interface in the presence of the oxygen vacancy. While the oxygen vacancy on the side of $SrTiO_3$ significantly lowers the Schottky barrier height, the oxygen vacancy close to the interface or inside the metallic electrode results in a Schottky barrier comparable to that of the clean interface. Based on these results, we propose a model for resistance-switching phenomena in perovskite oxide/metal interfaces where electromigration of the oxygen vacancy plays a key role. Our model provides a consistent explanation of a recent experiment on resistance switching in $SrRuO_3/Nb:SrTiO_3$ interface. © *2006 American Institute of Physics*. [DOI: 10.1063/1.2234840]

Reversible resistance-switching phenomena in transition metal oxides such as NiO,[1] TiO_2,[2] and $SrTiO_3$ (Refs. 3 and 4) have recently been receiving attention in both fundamental researches as well as commercial applications. Relatively simple metal-oxide-metal structures and good retention properties for resistance states could be exploited for a next generation nonvolatile memory device known as resistance-switching random access memory (ReRAM). However, there are many technical issues to be addressed before the actual commercialization of ReRAM devices, and most of them are related to the lack of fundamental understanding of the switching phenomena, especially at the microscopic level. Several phenomenological models have been proposed to date; charge trap model,[5] conducting domain model,[6] metallic filamentary path,[2] Mott transition,[7] and electrochemical migration of point defects.[8,9] Recently, based on a systematic study on the Schottky junction formed by metallic electrode of $SrRuO_3$ and *n*-type semiconductor of Nb-doped $SrTiO_3$, Fujii *et al.* claimed that the observed resistance switching can be understood through a variable Schottky barrier model.[10] An explanation at an atomistic level is yet to be found.

In this letter, based on the results from first-principles calculations, we propose a switching mechanism at the perovskite oxide/metal interface where the oxygen vacancy (V_O) plays a crucial role in changing a Schottky barrier height (ϕ_B) formed at the oxide/metal interface. For a computational package, we use Vienna *ab initio* simulation package (VASP).[11] We use projector-augmented-wave potentials[12] for describing electron-ion interactions and the energy cutoff for plane waves expanding electronic wave functions is set to 400 eV. For *k*-point sampling, $6\times6\times1$ and $3\times3\times1$ meshes are used for the clean and defective interface models, respectively. We employ the local density approximation for the exchange-correlation energy of electrons. For all calculations, we relax internal positions until Hellmann-Feynman forces are reduced to within 0.03 eV/Å.

Figure 1(a) is a schematic picture of the model system used in the present work. Our model system consists of four layers of $SrRuO_3$ epitaxially built on eight layers of $SrTiO_3$. The lattice parameters are matched to those of $SrTiO_3$. The lattice mismatch between $SrRuO_3$ and $SrTiO_3$ is less than 1% both experimentally and theoretically. Due to the periodic boundary condition required for plane-wave calcula-

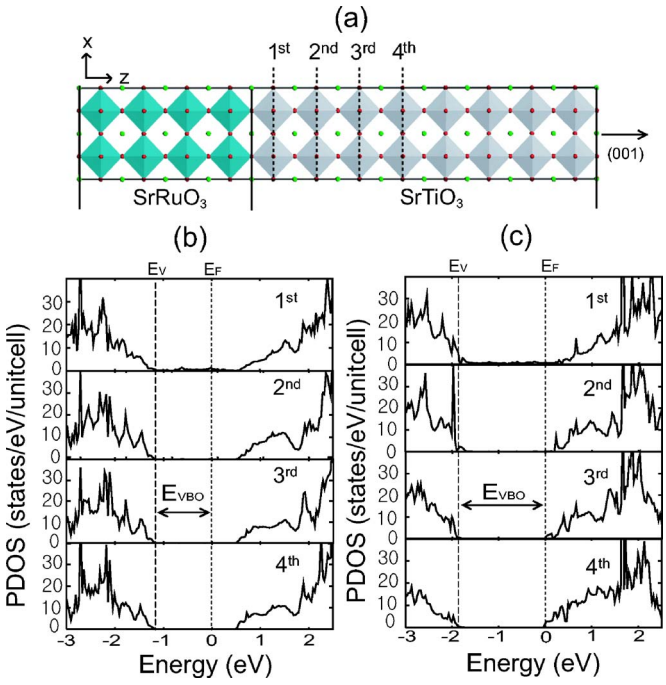

FIG. 1. (Color online) (a) A schematic picture of the unit cell of the model system. The shaded squares represent octahedra formed by oxygens. (b) Partial density of states (PDOS) for the clean interface, i.e., without any defect, projected onto each layer indicated in (a). (c) PDOS in a similar style with the oxygen vacancy present in the fourth TiO_2 layer in (a).

[a)]Authors to whom correspondence should be addressed.
[b)]Electronic mail: bhpark@konkuk.ac.kr
[c)]Electronic mail: hansw@ewha.ac.kr

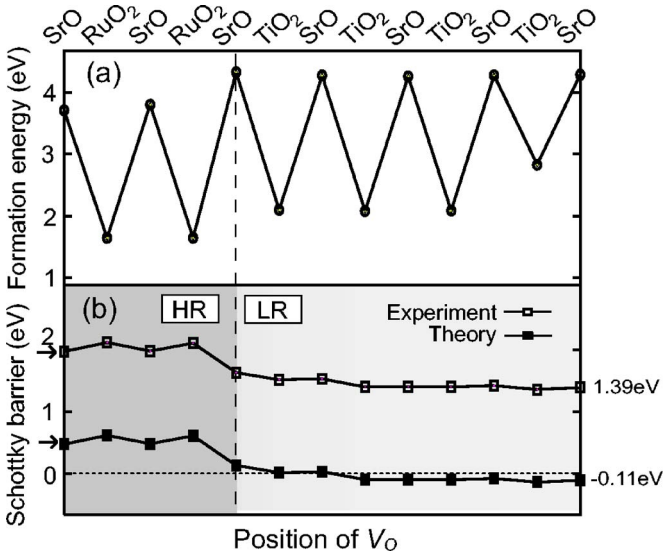

FIG. 2. (a) Comparison of defect formation energies between configurations with oxygen vacancies created in different layers (indicated at the top of the figure). The formation energy of V_O is evaluated as $E_{tot}(V_O)+\mu_O-E_{tot}(\text{clean})$, where E_{tot} is the total energy for defect-including and clean interfaces and μ_O is the chemical potential of an oxygen atom (set to the half of the total energy of O_2). The vertical dashed line indicates the interface between $SrRuO_3$ and $SrTiO_3$. (b) The change of ϕ_B as a function of the vacancy position. Each plot is drawn by assuming experimental (3.2 eV) or theoretical (1.7 eV) energy gap of $SrTiO_3$. The arrows at the left y axis indicate ϕ_B of the clean interface. HR and LR represent high and low resistance regions, respectively.

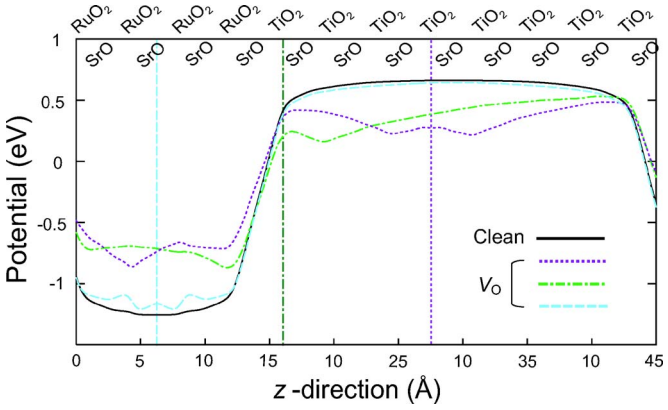

FIG. 3. (Color online) The macroscopically averaged local potential along the z direction for clean or defect-including interfaces. The corresponding position of V_O is indicated by a vertical line with the same line style. When V_O is inside $SrRuO_3$ (dashed line), the average potential is close to that of the clean interface (solid line).

tions, there are two symmetric metal/oxide interfaces formed in our model system.

We first estimate ϕ_B at the clean STO/SRO interface. In Fig. 1(b), we plot the partial density of state (PDOS) projected onto each TiO_2 layer indicated in Fig. 1(a). It can be observed that the valence-band offsets (E_{VBO}) from the Fermi level are similar from layer to layer, and ϕ_B for electron carriers can be directly defined as follows:

$$\phi_B = E_g - E_{VBO}, \tag{1}$$

where E_g indicates the energy gap of $SrTiO_3$ which is 1.72 eV (theory) or 3.2 eV (experiment). It is well known that the local density approximation underestimates the energy gap by 30%–40% and we assume that the error in the position of valence edge is much smaller than that for the conduction edge.[13] The ϕ_B estimated in this way is 0.37 eV (theory) or 1.85 eV (experiment). There is another widely used method of evaluating ϕ_B for a heterojunction using the macroscopic average of the local potential.[14] Applying this method to clean SRO/STO interface, we obtain ϕ_B of 0.67 eV (theory) or 2.15 eV (experiment) which is in reasonable agreement with direct evaluations from the PDOS. The small discrepancy of 0.3 eV can be ascribed to insufficient layers of $SrRuO_3$ in the model system.

Next we introduce V_O by removing an oxygen atom with a 2×2 lateral (xy) periodicity. This corresponds to a nominal stoichiometry of $SrTiO_{2.97}$. V_O in $SrTiO_3$ is known to result in the electron doping of the material by shifting the Fermi level into the conduction band.[15] The defect formation energies for different V_O configurations are presented in Fig. 2(a). The chemical potential of an oxygen atom is set to the half of the energy of the oxygen molecule. For comparison, the defect formation energy of V_O in the bulk is calculated to be 4.7 eV. It is found that V_O is more stable when it is located in TiO_2 or RuO_2 layers rather than SrO layers. This is related to the screening capability of the layer containing V_O which lowers spurious Coulomb energies around the vacancy site. We note, however, that the relative difference should depend on the V_O-V_O separation in the xy plane.

In Fig. 1(c), PDOS for each TiO_2 layer is shown when V_O is located at the fourth TiO_2 layer [see Fig. 1(a)]. Compared to the clean interface shown in Fig. 1(b), a rigid shift of PDOS is clearly noticeable. The PDOS shifts slightly from layer to layer, reflecting weak band bending. The valence edge is still well defined for each TiO_2 layer, allowing for a reasonable estimation of ϕ_B. On the other hand, the macroscopic average of local potential (see Fig. 3) does not exhibit a flat bottom to set the reference energy, which makes it difficult to assign ϕ_B on the basis of band lineup. Therefore, we rely on the direct extraction of E_{VBO} from PDOS, as was done for the clean interface. Since valence edges change layer to layer slightly due to a band-bending effect, we choose a band offset at the innermost layer, i.e., fourth TiO_2 layer in Fig. 1(a). The variation in ϕ_B is reminiscent of the Schottky limit of metal-semiconductor interface. This is consistent with the low density of interface states as found in Figs. 1(b) and 1(c).

In Fig. 2, we plot ϕ_B as a function of the vacancy position. Both experimental and theoretical energy gaps are considered in Eq. (1). It is noticeable that ϕ_B changes substantially depending on the position of V_O. When V_O is inside $SrRuO_3$ electrode, its effect on the potential is mostly screened due to the metallic property of $SrRuO_3$ and ϕ_B of the clean interface (indicated by arrows) is recovered. On the other hand, if V_O is away from the interface, ϕ_B is reduced down to −0.33 eV (theory) or 1.15 eV (experiment). The negative sign of theoretical ϕ_B means that the valence edge of $SrTiO_3$ is lower than the Fermi level of the metallic electrode. This is ascribed to the underestimation of energy gap in the local density approximation. In fact, it is found that one to two electrons are transferred from the metallic electrode to the dielectric. This increases the electronic potential in $SrTiO_3$, which has an effect of shifting up the valence edge of $SrTiO_3$ and hence ϕ_B. Therefore, we expect that reduction of ϕ_B in real materials would be greater than that observed in Fig. 2(b). One can divide SRO/STO interface into two regions in terms of the position of V_O; HR is the

high resistance region with ϕ_B comparable to that of the clean interface. LR is the low resistance region with lower ϕ_B or even Ohmic contact [see Fig. 2(b)].

Our observation of vacancy-dependent ϕ_B can explain a recent experimental observation of hysteretic *I-V* characteristics of the Schottky junction formed at SRO/Nb:STO interface.[10] In that work, a forward bias scan drove the junction to low resistance state while the reverse bias scan resulted in high resistance states. Based on our computational results, this can be explained in terms of electromigration of V_O; oxygen vacancies are easily generated in Nb-doped $SrTiO_3$ due to high growth temperatures.[16] Since the effective charge of V_O is positive, the forward bias (or positive voltage at electrode) will drive V_O away from the interface or into LR in Fig. 2(b). The opposite thing will occur for a reverse bias scan and V_O now moves into HR. With the increase of the extreme value of each bias scan, the chance of electromigration of V_O also increases, resulting in a larger variation of ϕ_B. This is in qualitative agreement with the experiment. On the other hand, V_O may not be able to move easily into $SrRuO_3$ due to the metallic screening. Therefore, a reverse bias larger than the forward bias will be required to drive V_O into the electrode, also consistent with the experiment.

An explanation about the time scale of electromigration of V_O in actual devices is in demand. The migration barrier of V_O in the bulk $SrTiO_3$ was measured to be 0.67–1.27 eV (Ref. 17) and we also obtain 0.6 eV using the nudged-elastic-band method.[18] A rough estimation gives $\geqslant$10 ms for a single hopping event of V_O at 300 K (see below), in contrast with the experiment in Ref. 10 where the switching behavior was observed for a pulse duration as small as 1 μs. This strongly implies that the electrical bias should lower the migration barrier substantially. The first-principles description of V_O migration at the biased metal/oxide interface is beyond the scope of this work. Instead, we estimate the migration time based on a simplified model of local environments at the interface. We first note that the depletion length at the SRO/Nb-STO interface would be very small since Nb-doped $SrTiO_3$ is a good conductor. Using a formula known for the metal-semiconductor interface,[19] the depletion length is estimated to be 5–10 nm from the interface. (The electric-field dependence of the dielectric constant of $SrTiO_3$ is also accounted for.) As the voltage drop occurs only along this narrow width, a large electric field will be applied in the depletion region. As a specific case, 10 V bias will result in an electric field of 1–2 V/nm, which decreases the activation energy approximately by 0.2–0.4 eV since V_O carries a nominal charge of $+2|e|$ (or oxygen carries $-2|e|$). Within the harmonic transition state theory, the average migration time τ is given by $\tau=1/[\nu\exp(-E_a/k_BT)]$, where ν is the attempt frequency and E_a is the activation energy. With $\nu\sim1$ THz, which is a typical frequency of soft mode in $SrTiO_3$, the migration time at 300 K lies in the range of nanosecond to microsecond which are far shorter than $\sim$10 ms for the unbiased case. This is in reasonable agreement with the experiment in Ref. 10 where the switching behavior was observed at 300 K as long as the time duration of 10 V pulse was longer than 1 μs.

For a microscopic understanding of ϕ_B variation, we look into the macroscopic average of the local potential in the presence of V_O, as shown in Fig. 3. It is noticeable that V_O lowers the local potential around the vacancy site. This leads to a rigid downshift of local electronic structures. Accordingly, the conduction edge of the dielectric moves closer to the Fermi level that is mostly determined by the metallic electrode. On the other hand, when V_O is in close proximity of the interface or inside the electrode, free electrons screen the positive potential of V_O and the potential profile of the clean interface recovers.

In summary, we have presented a resistance-switching model based on first-principles calculations on SRO/STO interface containing V_O. The change of ϕ_B as dictated by the electromigration of V_O in response to the external bias was found to provide a consistent explanation of a recent experimental report. Although we employed a specific model of SRO/STO interface, our results also have implications for other metal/perovskite interfaces.[8,20]

This work was supported by National Research Program for the 0.1 Terabit Nonvolatile Memory Development sponsored by MOCIE and KOSEF through National Research Laboratory (NRL) program. The computations were carried out at KISTI through Seventh Strategic Supercomputing Program.

[1] S. Seo, M. J. Lee, D. H. Seo, E. J. Jeoung, D.-S. Suh, Y. S. Joung, I. K. Yoo, I. R. Hwang, S. H. Kim, I. S. Byun, J.-S. Kim, J. S. Choi, and B. H. Park, Appl. Phys. Lett. **85**, 5655 (2004).
[2] C. Rohde, B. J. Choi, D. S. Jeong, S. Choi, J. S. Zhao, and C. S. Hwang, Appl. Phys. Lett. **86**, 262907 (2005).
[3] Y. Watanabe, J. G. Bednorz, A. Bietsch, Ch. Gerber, D. Widmer, A. Beck, and S. J. Wind, Appl. Phys. Lett. **78**, 3738 (2001).
[4] A. Beck, J. G. Bednorz, Ch. Gerber, C. Rossel, and D. Widmer, Appl. Phys. Lett. **77**, 139 (2000).
[5] J. G. Simmons and R. R. Verderber, Proc. R. Soc. London, Ser. A **301**, 77 (1967).
[6] M. J. Rozengerg, I. H. Inoue, and M. J. Sanchez, Phys. Rev. Lett. **92**, 178302 (2004).
[7] R. Fors, S. I. Khartsev, and A. M. Grishin, Phys. Rev. B **71**, 045305 (2005).
[8] A. Baikalov, Y. Q. Wang, B. Shen, B. Lorenz, S. Tsui, Y. Y. Sun, and Y. Y. Xue, Appl. Phys. Lett. **83**, 957 (2003).
[9] K. Szot, W. Speier, G. Bihlmayer, and R. Waser, Nat. Mater. **5**, 312 (2006).
[10] T. Fujii, M. Kawasaki, A. Sawa, H. Akoh, Y. Kawazoe, and Y. Tokura, Appl. Phys. Lett. **86**, 012107 (2005).
[11] G. Kresse and J. Hafner, Phys. Rev. B **47**, 558(R) (1993); **49**, 14251 (1994).
[12] P. E. Blöchl, Phys. Rev. B **50**, 17953 (1994).
[13] J. Junquera, M. Zimmer, P. Ordejon, and P. Ghosez, Phys. Rev. B **67**, 155327 (2003).
[14] R. G. Dandrea and C. B. Duke, J. Vac. Sci. Technol. A **11**, 848 (1993).
[15] W. Gong, H. Yun, Y. B. Ning, J. E. Greedan, W. R. Datans and C. V. Stager, J. Solid State Chem. **90**, 320 (1991).
[16] S. H. Kim, J. H. Moon, J. H. Park, J. G. Park, and Y. H. Kim, J. Mater. Res. **16**, 192 (2001).
[17] A. E. Paladino, L. G. Rubin, and J. S. Waugh, J. Phys. Chem. Solids **26**, 391 (1965); A. Yamaji, J. Am. Ceram. Soc. **58**, 152 (1975).
[18] G. Henkelman and H. Jónsson, J. Chem. Phys. **113**, 9978 (2000).
[19] S. M. Sze, *Physics of Semiconductor Devices*, 2nd ed. (Wiley, New York, 1981).
[20] A. Sawa, T. Fujii, M. Kawasaki, and Y. Tokura, Appl. Phys. Lett. **85**, 4073 (2004).